Analysis of the parametrically periodically driven classical and quantum linear oscillator

Vladimir Grubelnik* and Marjan Logar
Faculty of Electrical Engineering and Computer Science, University of Maribor, Koroška cesta 46, SI-2000 Maribor, Slovenia, European Union

Marko Robnik†
CAMTP-Center for Applied Mathematics and Theoretical Physics, University of Maribor, Mladinska 3, SI-2000 Maribor, Slovenia, European Union and Department of Mathematics, Huaqiao University, Quanzhou, 362000, China

Yonghui Xia‡
Department of Mathematics, Zhejiang Normal University, Jinhua, 321004, China

(Received 5 June 2018; revised manuscript received 15 January 2019; published 13 February 2019)

We study theoretically and computationally the behavior of the classical and quantum parametrically periodically driven linear oscillator. As a basic paradigm of such a Floquet system we consider the case of the harmonic oscillation of the oscillator frequency, which is convenient to handle theoretically and computationally, while keeping the general features. We derive an explicit analytic formula for the quantum propagator in terms of the classical propagator. Using this, we derive the explicit exact formula for the evolution of the expectation value of the energy starting from an arbitrary normalizable initial state. In the case of the starting pure stationary eigenstate the evolution is exactly the same as for the classical microcanonical ensemble of initial conditions of the same starting energy. We perform a rather complete computational analysis of the system's behavior inside the instability regions (lacunae), where the energy of the oscillator increases exponentially, as well as in the stability regions, and in particular in the vicinity of the (in)stability borders. We confirm also numerically with absolute certainty that the borders of (in)stability regions classically and quantally coincide *exactly*, in accordance with the theory, which is an important check of the numerical accuracy of computations, and we find a number of important empirical results, especially an equation of the elliptic type describing the rate of exponential energy growth inside the lacunae in terms of other systems' quantities. We believe that our approach and findings are of generic linear type, i.e., applicable in most such linear Floquet systems, and we present a strong motivation for a general theory, classically and quantally.

DOI: 10.1103/PhysRevE.99.022209

I. INTRODUCTION

Time-dependent Hamilton systems [1–5] are important when the interaction of a given Hamilton system with the environment is modeled and analyzed. Formally, they can be reduced to an autonomous (time-independent) system by introducing one more dimension in phase space (so-called extended phase space) or one more degree of freedom, but technically they are more easily studied as time-dependent systems, because we have a number of techniques which lead directly to deep physical insights and mathematical methodological advantages. Such systems have been the subject of many recent studies, both classically [6–12] and quantally [13–16]. In particular, we should mention works on one-dimensional quantum billiards [17–21], in particular the work by Seba [22] and our recent paper [16], as well as the two-dimensional quantum billiards [23–26]. Fermi acceleration (FA; by definition it means unlimited and unbounded growth of the particle's energy, subject to the time-dependent potential) is of central interest [27,28]. While FA is certainly possible in two-dimensional or higher-dimensional classical Hamilton systems, like billiards [13], even in the case of a smooth periodic driving (motion of the boundary), it cannot occur in one-dimensional box so long as the oscillation is smooth and the KAM theorem applies, as it predicts existence of invariant curves acting as perfect barriers in the classical phase space [29]. However, if the periodic oscillation of the wall is not smooth enough, like the sawtooth type of oscillation, the KAM theorem does not apply and the route to FA is open, which indeed has been studied in references [22,30,31]. The quantum mechanical FA indeed can take place [16], and it turns out that the energy grows quadratically with time in very narrow quantum resonant gaps.

In this paper we study the periodically parametrically driven linear oscillator, both classically and quantally. While the classical problem is a text book example (see, e.g., Ref. [1]), which, however, is difficult to study analytically and rigorously [32], the quantum problem is entirely unsolved analytically, although a special case of such a Floquet system has been analyzed rigorously by Weigert [33].

*vlado.grubelnik@um.si
†Robnik@uni-mb.si
‡xiadoc@163.com

In our case the frequency (*not* the square of the frequency) of the linear oscillator is assumed to vary harmonically, $\omega(t) = 2\pi(1 + \varepsilon \cos \Omega t)$, which greatly simplifies the quantum computations while keeping the general aspects of the parametric resonance. The control parameter space has two dimensions, the frequency of the parametric driving Ω and its amplitude ε. Our main result is to precisely describe the instability regions (lacunae), showing that inside the lacunae the energy growth at large times is exponential with time, while it oscillates and is bounded outside the lacunae. The (in)stability border in the parameter space (Ω, ε) is shown to coincide *exactly* classically and quantally, which we explain theoretically (see below). This is certainly an important ultimate confirmation of numerical accuracy. Moreover, we derive explicit analytic formula for the quantum propagator in terms of the classical propagator. Using this, we derive the explicit exact formula for the evolution of the expectation value of the energy starting from an arbitrary normalizable initial state. In the case of the pure stationary eigenstate as initial state, the evolution is exactly the same as for the classical microcanonical ensemble of initial conditions of the same starting energy. Furthermore, we obtain a number of important empirical results, such as an equation of the elliptic type describing the rate of exponential energy growth inside the lacunae in terms of other system's quantities. The analysis of the detailed structure of the lacunae is typically very difficult, both theoretically and numerically; therefore, we believe that our approach and results contribute to the literature on this subject.

Here, some historical comments are in place. There is a vast literature on the classical and quantum Floquet systems. On the classical side we refer to Refs. [34–36], where the Hill's equation, and the Mathieu equation as its special case, are treated, and our system is a special case of the Hill's equation. The analysis there is in the configuration space, while we perform the analysis in the phase space (x, p), which certainly is a more direct approach. When classical and quantum mechanics of our system are compared one must bear in mind that the concept of an orbit emanating from a single initial condition (x, p) does not exist in the quantum mechanics. When we compare the propagation of classical and quantum states with a certain average energy we must consider a certain ensemble of classical orbits to be compared with the quantum state and its average energy. Thus the description is necessarily statistical. It is nontrivial to find such a correspondence.

In the literature (see, e.g., Ref. [37] and the references therein) it is known that the semiclassical motion and spreading of quantum wave packets follow the classical flow at least for some time (Ehrenfest time), where the spreading is exponential in the case of unstable orbits. In the bound Hamilton systems with quadratic momenta and coordinates (linear oscillators), there is no spreading and the center of the wave packet precisely follows the classical orbit in the phase space for all times. However, physically more interesting is the question how the energy of an initial stationary state (with prepared sharp energy) develops in time. We express the quantum propagator in terms of the classical propagator, and present an explicit formula in closed form for the energy [see Eqs. (16), (27), and (29)], as explained above, although the classical propagator cannot be calculated analytically in the general case. The analogy of a quantum stationary state is the classical microcanonical distribution of initial conditions with the same energy, and their developments are identical. To calculate the boundary of the stable and unstable regions in the parameter space (Ω, ε) we have to resort to numerical calculations, both classically and quantally, which we do in this paper with unprecedented accuracy, and confirm that they are identical, which is another confirmation of the accuracy of numerical calculations. In addition, we study also the dependence of the classical motion on the initial conditions.

The paper is organized as follows. In Sec. II we define the underlying quantum and classical system, and prepare the tools to describe its evolution in time. We derive the quantum propagator in terms of the classical propagator. In Sec. III we present the numerical method and carefully check the numerical routines to warrant the sufficient numerical accuracy. In Sec. IV we present the main results for the quantum case, by investigating the borders of lacunae, which are shown to coincide *exactly* with the borders of the classical lacunae, as explained theoretically. In Sec. V we analyze further details of the classical system. In Sec. VI we study the comparison between the classical and quantum system, and in Sec. VII we present some most important empirical (computational) results on the relations among the parameters characterizing the structure of the lacunae. In Sec. VIII we summarize our results, discuss open problems, and conclude.

II. DEFINITION OF THE SYSTEM AND THE PROBLEM

A. The quantum problem

We study a point particle of mass m moving in a time-dependent quadratic potential well (which is time-dependent linear oscillator), described by the Hamilton operator

$$\hat{H} = -\frac{1}{2}\frac{\partial^2}{\partial x^2} + \frac{1}{2}\omega^2(t)x^2, \tag{1}$$

where we always use the units such that $m = 1$, $\hbar = 1$. The classical analog is the Hamilton function

$$H = \frac{p^2}{2} + \frac{1}{2}\omega^2(t)x^2, \tag{2}$$

where the frequency $\omega(t)$ is a periodic function of time t. More specifically, in the entire paper we consider the following model:

$$\omega = \omega(t) = 2\pi(1 + \varepsilon \cos \Omega t), \tag{3}$$

which is more convenient to deal with than the usual Mathieu model $\omega^2(t) = (2\pi)^2(1 + \varepsilon \cos \Omega t)$, as we shall see. The control parameter space is thus (Ω, ε). We use units of time such that the period of the unperturbed oscillator ($\varepsilon = 0$) is equal to 1. We are seeking the solution $\psi(x, t)$ of the time-dependent Schrödinger equation ($\hbar = 1$),

$$\hat{H}\psi = i\frac{\partial \psi}{\partial t}. \tag{4}$$

To find it we use the expansion of the solution

$$\psi(x, t) = \sum_{n=0}^{\infty} b_n(t)u_n(x, t) \exp\left[-i\int_0^t E_n(\tau)d\tau\right] \tag{5}$$

in terms of the *adiabatic basis*, namely, in terms of the instantaneous eigenbasis

$$u_n(x,t)=\frac{1}{\sqrt{2^n n!}}\left(\frac{\omega(t)}{\pi}\right)^{\frac{1}{4}}\exp\left(-\frac{\omega(t)x^2}{2}\right)\mathcal{H}_n[x\sqrt{\omega(t)}]. \tag{6}$$

Here $\mathcal{H}_n(s)$ is the nth Hermite polynomial of s and we have the orthonormality of the (for any time t) complete basis $\langle u_m|u_n\rangle=\delta_{m,n}$ (Kronecker δ function), where

$$\hat{H}u_n=E_n u_n,\quad E_n=\left(n+\tfrac{1}{2}\right)\omega(t)=E_n(t),\quad n=0,1,2,3,\ldots. \tag{7}$$

Inserting the ansatz Eqs. (5) into (4) and taking the scalar product with u_m we get

$$\dot{b}_m=-\sum_{n=0}^{\infty}b_n\langle u_m|\dot{u}_n\rangle\exp\left\{-i\int_0^t[E_n(\tau)-E_m(\tau)]d\tau\right\}, \tag{8}$$

where the dot denotes the time derivative. Using the well known properties of the Hermite polynomials we find

$$\dot{u}_n=\frac{1}{4\omega}\dot{\omega}u_n-\frac{x^2}{2}\dot{\omega}u_n+\sqrt{\frac{n}{2\omega}}\dot{\omega}xu_{n-1}. \tag{9}$$

Now inserting this into Eq. (8) and then using the matrix elements, which are easy to verify,

$$\langle m|x|n-1\rangle=\frac{1}{\sqrt{2\omega}}(\sqrt{m+1}\delta_{m,n-2}+\sqrt{m}\delta_{m,n}), \tag{10}$$

and

$$\langle m|x^2|n\rangle=\frac{1}{2\omega}(\sqrt{(m+1)(m+2)}\delta_{m,n-2}+(2m+1)\delta_{m,n}+\sqrt{m(m-1)}\delta_{m,n+2}), \tag{11}$$

we arrive at the final equations of motion for the expansion coefficients $b_m(t)$, namely,

$$\dot{b}_m=-\frac{\dot{\omega}}{4\omega}\left\{b_{m+2}\sqrt{(m+1)(m+2)}\exp\left[-2i\int_0^t\omega(\tau)d\tau\right]-b_{m-2}\sqrt{m(m-1)}\exp\left[+2i\int_0^t\omega(\tau)d\tau\right]\right\}. \tag{12}$$

Here $\omega(t)$ is still of general form. By writing the evolution of b in operator (or matrix) form $b=Bb_i$, using the evolution equation $\dot{B}=AB$, and b_i being an arbitrary initial state vector $b_i=\{b_n(t=0)\}$, and assuming that the matrix A is antihermitian, $A^\dagger=-A$, we can see that the probability $\langle b|b\rangle=\sum_{m=0}^{M}|b_n|^2$ is conserved for any dimension M of A and B, that is also for truncated systems of any size. Indeed, we can see that our Eqs. (12) are exactly of this type.

In continuation, we see now that the integral $\int_0^t\omega(\tau)d\tau$ can be evaluated analytically in elementary form for our model Eq. (3), which leads then to the final equations specific of our model

$$\dot{b}_m=\frac{\varepsilon\ \Omega\sin\Omega t}{4(1+\varepsilon\cos\Omega t)}\left\{b_{m+2}\sqrt{(m+1)(m+2)}\times\exp\left[-4\pi i\left(t+\frac{\varepsilon}{\Omega}\sin\Omega t\right)\right]-b_{m-2}\sqrt{m(m-1)}\times\exp\left[+4\pi i\left(t+\frac{\varepsilon}{\Omega}\sin\Omega t\right)\right]\right\}. \tag{13}$$

We are primarily interested in the development of the mean (expected) energy $E(t)$ as a function of time,

$$E(t)=2\pi(1+\varepsilon\cos\Omega t)\sum_{m=0}^{\infty}|b_m|^2\left(m+\frac{1}{2}\right). \tag{14}$$

Moreover, in all numerical quantum calculations in the paper we shall start from the initial condition that at time $t=0$ the system is in the ground state $m=0$, that is $b_0=1$ and $b_m=0$ for all $m>0$, and $E(0)=\pi(1+\varepsilon)$. This is certainly enough, as the probability always moves to higher excited states, so that asymptotic behavior of the system and its energy $E(t)$ is the same for any starting initial state m.

B. The classical problem

On the basis of classical parametric resonance at $\varepsilon=0$ [38] we expect the corresponding quantum parametric resonance also at $\Omega=\Omega_n=4\pi/n$, where $n=1,2,3,\ldots$, and the energy $E(t)$ is expected to grow exponentially. This is indeed confirmed in our computations, as we shall see in the detailed analysis of Sec. IV. The theoretical explanation is given below in Sec. II C.

Let us write down the classical equations of motion, using Eq. (2),

$$\dot{p}=-\frac{\partial H}{\partial x}=-\omega^2(t)x,\quad \dot{x}=\frac{\partial H}{\partial p}=p, \tag{15}$$

where a solution of $\ddot{x}+\omega^2(t)x=0$ will be denoted by $w(t)$. The phase flow map Φ is linear and area preserving,

$$\begin{pmatrix}x(t)\\p(t)\end{pmatrix}=\begin{pmatrix}a,&b\\c,&d\end{pmatrix}\begin{pmatrix}x(0)\\p(0)\end{pmatrix}=\Phi\begin{pmatrix}x(0)\\p(0)\end{pmatrix}, \tag{16}$$

which means $\mathrm{Det}\Phi=ad-bc=1$. If $w_1(t)$ and $w_2(t)$ are two linearly independent solutions of the Eq. (15), then we can define the Wronskian matrix Ψ as

$$\Psi(t)=\begin{pmatrix}w_1(t),&w_2(t)\\\dot{w}_1(t),&\dot{w}_2(t)\end{pmatrix} \tag{17}$$

and we easily see that

$$\Phi(t)=\Psi(t)\Psi^{-1}(0) \tag{18}$$

and verify $\mathrm{Det}\Phi=1$, because the Wronskian determinant $\mathrm{Det}\Psi(t)$ is constant as is well known. Let us denote the Floquet propagator by $\Phi_1=\Phi(T)$, where $T=2\pi/\Omega$ is the period of parametric driving. Then $\Phi(NT)$, N being an integer number, is equal to Φ_1^N. Thus, the stability of our system is entirely determined by the eigenvalues λ of Φ_1, namely,

$$\lambda^2-\lambda\ \mathrm{Tr}\Phi_1+1=0, \tag{19}$$

where $\mathrm{Tr}\Phi_1 = a + d$, with the solution

$$\lambda = \tfrac{1}{2}(\mathrm{Tr}\Phi_1 \pm \sqrt{(\mathrm{Tr}\Phi_1)^2 - 4}). \tag{20}$$

If $|\mathrm{Tr}\Phi_1| \geqslant 2$ we have instability, and exponential growth of the solution and of the energy, while for $|\mathrm{Tr}\Phi_1| < 2$ we have stability, a bounded oscillatory motion.

To study the stability properties of the system for the given values of the control parameters (Ω, ε) we use the following procedure. Set the initial conditions $(x_0 = 1,\ p_0 = 0)$ and integrate numerically up to time T, and denote $(w_1(T),\ \dot{w}_1(T)) = (x(T),\ p(T))$. Then set the initial conditions $(x_0 = 0,\ p_0 = 1)$ and integrate numerically up to time T, and denote $(w_2(T),\ \dot{w}_2(T)) = (x(T),\ p(T))$. Then we see that $\Psi(0)$ is identity matrix

$$\Psi(0) = \begin{pmatrix} 1, & 0 \\ 0, & 1 \end{pmatrix} \tag{21}$$

and therefore $\Phi_1 = \Phi(T) = \Psi(T)$, and $\mathrm{Tr}\Phi_1 = \mathrm{Tr}\Psi(T) = w_1(T) + \dot{w}_2(T)$. Thus, finally the instability criterion is

$$|\mathrm{Tr}\Phi_1| = |w_1(T) + \dot{w}_2(T)| \geqslant 2, \quad T = \frac{2\pi}{\Omega}. \tag{22}$$

This is the method that we use to numerically solve the classical problem, which should be compared with the approach by McLachlan [34].

C. The relation between the quantum and the classical problem

In this subsection we show the relationship between the classical and quantum evolution of the energy, namely, that the instability criterion is exactly the same in both cases, and moreover, that the evolution of the expectation value of the quantum energy starting from initial pure stationary eigenstate is the same as the evolution of the classical energy when averaged over a microcanonical ensemble of the initial conditions at the same energy.

The key insight is the observation that the quantization commutes with linear canonical transformations. Time evolution of a Hamilton system is a canonical transformation, and it is linear for the linear oscillator. Therefore, the Eqs. (16) apply also to the quantum operators.

We are interested in the expectation value of the energy, denoted by $E(t)$, at time t as described by the current state (wavefunction) $\psi(t)$ at time t,

$$E(t) = \langle \psi(t)|\hat{H}(t)|\psi(t)\rangle, \tag{23}$$

where $\hat{H}(t)$ is the operator Eq. (1). The current state $\psi(t)$ is evolved from the initial state denoted by ψ_0 by a unitary propagator $\hat{U}(t)$, namely, $\psi(t) = \hat{U}(t)\psi_0$. Then, we can write

$$E(t) = \langle \psi_0|\hat{U}^{-1}(t)\hat{H}(t)\hat{U}(t)|\psi_0\rangle \tag{24}$$

and we identify the operator

$$\hat{H}_0 = \hat{U}^{-1}(t)\hat{H}(t)\hat{U}(t) \tag{25}$$

where $\hat{H}_0$ is now determined by the linear canonical transformation Eq. (16), and $\hat{x}_0$ and $\hat{p}_0$ are operators acting on $\psi_0 = \psi(0)$ as a function of $x_0 = x(0)$. Explicitly, we find

$$\hat{H}_0 = \tfrac{1}{2}(d^2 + \omega^2 b^2)\hat{p}_0^2 + \tfrac{1}{2}(\hat{x}_0\hat{p}_0 + \hat{p}_0\hat{x}_0)(cd + \omega^2 ab) + \tfrac{1}{2}(c^2 + \omega^2 a^2)\hat{x}_0^2. \tag{26}$$

For the initial state $\psi_0(x_0)$, which can be expanded in the basis Eq. (6) with real expansion coefficients, we get [because the mixed type terms emanating from the operator $(\hat{x}_0\hat{p}_0 + \hat{p}_0\hat{x}_0)$ must vanish then, if $\psi_0(x_0)$ is real]

$$E(t) = \frac{1}{2}(d^2 + \omega^2(t)b^2)\int_{-\infty}^{\infty}\left|\frac{d\psi_0}{dx_0}\right|^2 dx_0 + \frac{1}{2}(c^2 + \omega^2(t)a^2) \times \int_{-\infty}^{\infty} x_0^2|\psi_0|^2 dx_0. \tag{27}$$

We shall always choose a pure eigenstate Eq. (6) as initial condition at time $t = 0$, thus $\psi(t = 0) = \psi_0(x_0) = u_n(x_0)$, namely,

$$u_n(x_0) = \frac{1}{\sqrt{2^n n!}}\left[\frac{\omega(0)}{\pi}\right]^{\frac{1}{4}} \exp\left[-\frac{\omega(0)x_0^2}{2}\right]\mathcal{H}_n[x_0\sqrt{\omega(0)}]. \tag{28}$$

Taking this into account it is straightforward to evaluate $E(t) = \langle u_n|\hat{H}_0|u_n\rangle$ in Eq. (27) with the result

$$E(t) = \frac{\omega_0\left(n + \frac{1}{2}\right)}{2}\left[\frac{c^2}{\omega_0^2} + a^2\frac{\omega^2(t)}{\omega_0^2} + d^2 + \omega^2(t)b^2\right], \tag{29}$$

where $\omega_0 = \omega(0)$. This result is identical to the classical result if we identify $E(0) = (n + \frac{1}{2})\omega_0$ with the energy of the classical microcanonical ensemble of initial conditions, over which we average, as calculated for time dependent linear oscillators by Robnik and Romanovski [39–41]. We remark that in the case of no time dependence $\omega(t) = \omega_0 = \text{const.}$ we have $a = \cos(\omega_0 t)$, $b = \omega_0^{-1}\sin(\omega_0 t)$, $c = -\omega_0\sin(\omega_0 t)$, $d = a = \cos(\omega_0 t)$ and therefore $E(t) = E(0) = (n + \frac{1}{2})\omega_0$. In the adiabatic case of very slow variation of $\omega(t)$ we find [39–41] $E(t) = \omega(t)(n + \frac{1}{2})$, in agreement with the quantum and classical adiabatic theorem.

Therefore, in the time periodic case of our Floquet problem, it is clear from Eq. (29) that the instability of classical motion, giving rise to the exponential increase of the energy, will exactly coincide with the quantum instability, where any of the classical flow map Φ coefficients a, b, c, d grows exponentially. Moreover, it is clearly seen from Eq. (27) that the same conclusion is true for any normalizable initial state $\psi_0(x_0)$, if the two integrals exist: The quantum evolution is unstable exactly when the classical motion is unstable.

To identify the stability and instability regions and the boundary between them, numerical calculations are necessary, as analytically we cannot solve exactly for the classical propagator Φ, its matrix elements a, b, c, d, and also the quantum formalism does not allow us to solve the problem analytically. This is typical for the Floquet-type problems. To have more complete understanding of the system, we have performed both the quantum and the classical calculations and compared them.

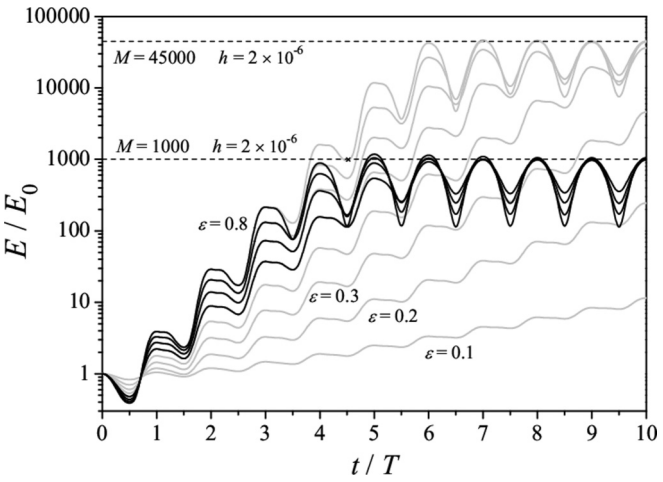

FIG. 1. The energy $E(t)$ in units of the initial energy $E(t=0) = E_0$ as a function of time in units of $T = 2\pi/\Omega = 1/2$ (the main resonance $\Omega = 4\pi$), for various values of $\varepsilon = 0.1, \ldots, 0.8$ in steps of ε equal to 0.1 for $M = 45\,000$ (gray), and for $M = 1000$ for $\varepsilon = 0.5, 0.6, 0.7, 0.8$ (black), in both cases with the integration step $h = 2 \times 10^{-6}$.

III. NUMERICAL METHOD AND PRELIMINARY RESULTS

Since our results and conclusions are based on the numerical calculations, it is necessary to implement and justify the appropriate method. In fact, we have used the same method as in our previous paper [16]. This section is devoted to the aspects of numerical technique.

To have a very good control over the numerical integration we have decided to use the fixed-step method rather than the methods with an adaptive stepsize.

We have implemented the Runge-Kutta integration method of 4th order in integrating the differential Eqs. (13) and (15). Of course, we had to cut off the vector b_m at certain maximal $m = M$. When we do that, we must verify that the contribution of the Mth term $b_M(t)$ to the energy equal to $2\pi(1+\cos\Omega t)|b_M|^2(M+\frac{1}{2})$ is sufficiently small to neglect it, as well as for all higher terms $m > M$, which justifies the truncation of the system at $m = M$. Also, the integration step must be carefully adapted to secure the numerical accuracy and at the same time to allow us to go to the large time scales of up to several hundreds or even thousands of periods of length $T = 2\pi/\Omega$. One of the necessary conditions to verify the numerical accuracy is the preservation of the total probability $\langle b|b\rangle = \sum_{m=0}^{M} |b_m|^2$. This has always been satisfied up to an error of at least the order 10^{-6} or better/smaller. The calculations have been performed even up to $M = 45\,000$ in which case the total probability decreased only by 10^{-7} after integration time $4T$.

We have also performed the reversibility test. Our initial condition is the fully occupied ground state $m = 0$, i.e., $b_0(0) = 1$ and $b_m(0) = 0$ for $m > 0$, as explained in the end of the Sec. II A. For $\varepsilon = 0.4$ and $M = 1000$ we have integrated the Eqs. (13) from $t = 0$ to $t = T$, and then back to $t = -T$ with the integration step $h = 2 \times 10^{-4}$. The results for the energy $E(t)$ at $t = 0$ as well as at $t = -T$ were reproduced within a numerical error of order 10^{-10}.

Finally, we did the convergence test, by increasing the truncation index M and making sure that the results of smaller M for the energy are sufficiently accurately reproduced. This is shown in Fig. 1 where we plot the energy $E(t) = H(t)$ in units of the initial energy $E(t=0) = E_0$ as a function of time in units of T. The main resonance frequency $\Omega = \Omega_1 = 4\pi$ is chosen. We have done the integrations for various values of $\varepsilon = 0.1, \ldots, 0.8$ in steps of 0.1 for $M = 45\,000$ (gray), and for $M = 1000$ for $\varepsilon = 0.5, 0.6, 0.7, 0.8$ (black), in both cases with the integration step $h = 2 \times 10^{-6}$. We can conclude that the results are numerically, and thus physically reliable, for E/E_0 up to several 1000. In this plot of $\log_{10}(E/E_0)$ versus time t/T we clearly see the exponential increase of $E(t)$.

IV. THE BORDERS OF THE INSTABILITY REGIONS (LACUNAE)

The main result of this paper is the analysis and description of the dynamical instability regions (lacunae) in the control parameter space (Ω, ε). Inside lacunae we have exponential

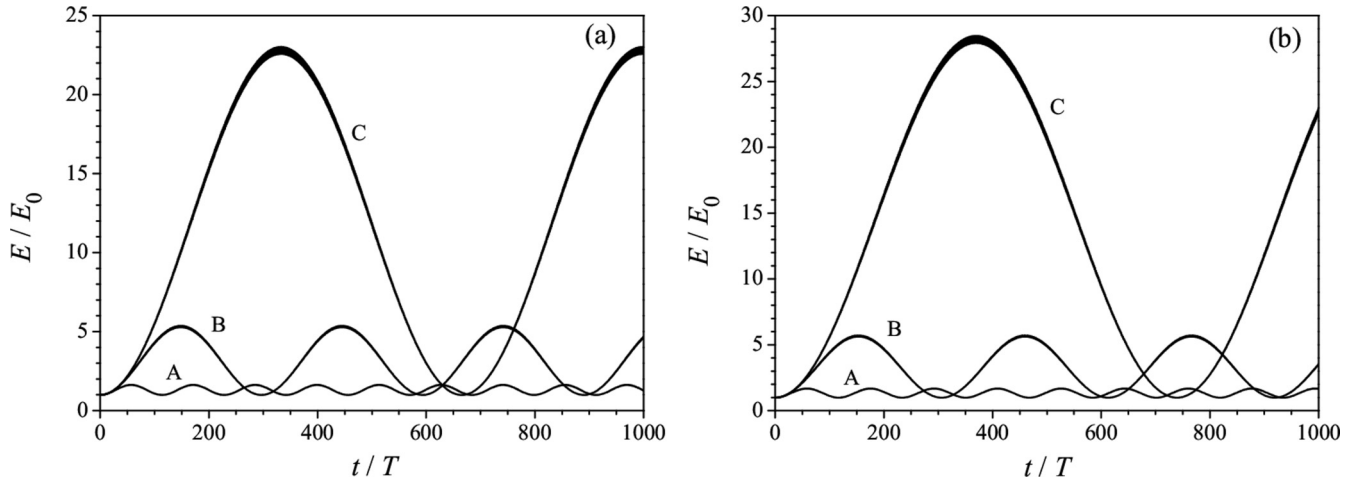

FIG. 2. The energy $E(t)/E_0$ vs. time t/T at fixed $\varepsilon = 0.01$, $M = 200$, and $n = 1$, for k from below $k < k^- = 0.99501889 \pm 10^{-8}$ in (a): (A) k=0.9900, (B) 0.9940, (C) 0.9948; and from above $k > k^+ = 1.00501862 \pm 10^{-8}$ in (b): (A) 1.0100, (B) 1.0060, (C) 1.0052.

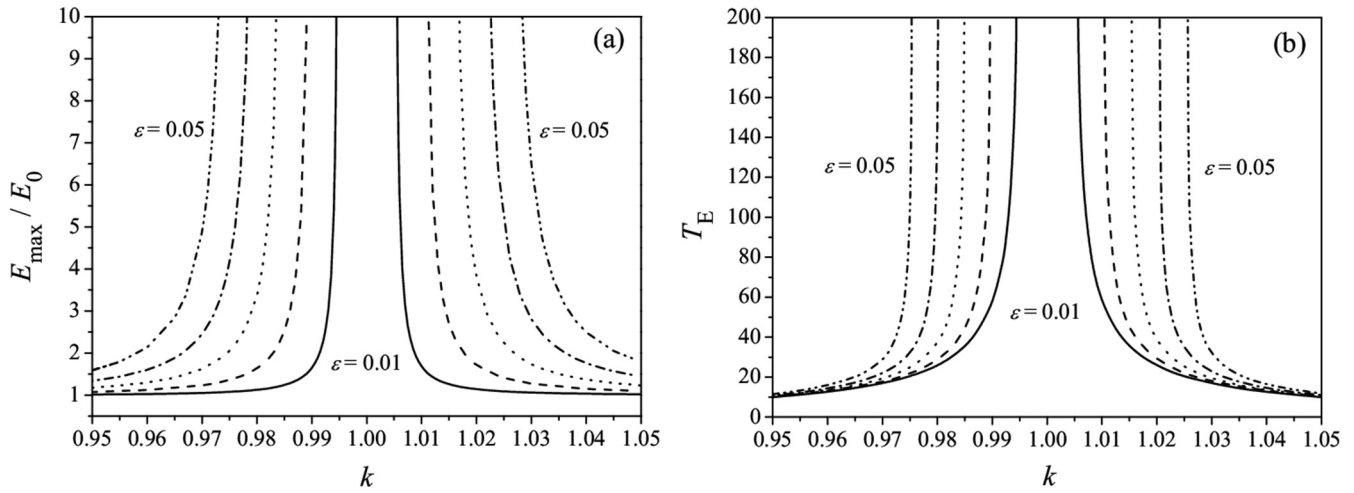

FIG. 3. The energy oscillation amplitude E_{max}/E_0 vs. k for the first lacuna $n = 1$ in (a) and the oscillation period T_E in (b) for $\varepsilon = 0.01, \ldots, 0.05$. $M < 5000$.

growth of $E(t)$ quantally [Eq. (14)] (for any initial condition) and classically (for all initial conditions except when (x_0, p_0) is exactly in the direction of the stable eigenvector of Φ), while outside the lacunae the energy oscillates with time (cf. Ref. [35]). Moreover, we shall demonstrate that the borders of the lacunae in (Ω, ε) classically and quantally *exactly* coincide, as explained in the Sec. II C. Therefore, for $\varepsilon = 0$ we expect [38] that the (parametric) resonance occurs for $\Omega_n = 4\pi/n$, where $n = 1, 2, 3, \ldots$, as is well known classically [1], and entirely confirmed below. For $\varepsilon \neq 0$ we must solve numerically the dynamical Eqs. (13), and (15), as analytic results so far are impossible, although the WKB analysis might be a successful approach in the future [32].

The method of detecting the instability region rests upon the observation that the energy $E(t)$ oscillates outside lacunae and is characterized by the fact that both the amplitude of oscillations and the oscillation period increase and diverge as we approach the instability border in (Ω, ε). Such a behavior is demonstrated in Fig. 2. By k we denote $k = \Omega/\Omega_n$,

$$k = \frac{\Omega}{\Omega_n}, \quad \Omega_n = \frac{4\pi}{n}. \tag{30}$$

Thus, at $\varepsilon = 0$, $k = 1$ is the border for all lacunae ($n = 1, 2, \ldots$). For a given $\varepsilon > 0$ we shall find a lower border $k^- < 1$ and the upper border $k^+ > k^-$ of the lacuna of nth order. The lacunae do not overlap, according to our experience. In Fig. 2 we show for the first lacuna $n = 1$, how the quantum energy $E(t)/E_0$ (14) oscillates with time t/T as we approach the border with k from below $k < k^-$ and from above $k > k^+$, at fixed $\varepsilon = 0.01$.

In Fig. 3 we show how the oscillation amplitude of the energy E_{max}/E_0 and the oscillation period T_E diverge as we approach the border of the first lacuna ($n = 1$) for various $\varepsilon = 0.01, \ldots, 0.05$.

As announced above, the borders of lacunae coincide classically and quantally, *exactly*. Classically, the border of lacunae is determined by the equality in Eq. (22), $|\mathrm{Tr}\Phi_1| = 2$. The results are presented graphically for the first four lacunae in Fig. 4, where the abscissa is $(4\pi/\Omega)^2$, which means that at $\varepsilon = 0$ and at the resonance frequency $\Omega_n = 4\pi/n$ we have $(4\pi/\Omega)^2 = n^2$, for $n = 1, 2, 3, 4$. The structure of the instability diagram is qualitatively in agreement with the general theory of the Hill's equation as exposed in Theorems 2.1 and 2.11–2.13 in Ref. [35]. It should be observed that on the borders of the odd n lacunae we have $\mathrm{Tr}\Phi_1 = -2$, while for even n we have $\mathrm{Tr}\Phi_1 = 2$. The more precise structure of each lacuna for $\varepsilon \leqslant 0.8$ on a smaller frequency interval around Ω_n, $n = 1, 2, 3, 4$ is shown in Fig. 5. Some more interesting details of the structure of the (in)stability borders are shown by zooming-in in Fig. 6 on much smaller frequency intervals of $k = \Omega/\Omega_n$ and for smaller values of ε.

Our finding is that inside lacunae we have for classical and quantal system the exponential growth of the energy both classically and quantally, and the bounded oscillatory behavior outside lacunae, in both cases very similar. To demonstrate that, we show in Fig. 7 for the first lacuna $n = 1$ the amplitude of the energy oscillation E_{max}/E_0 as a function of $k = \Omega/\Omega_1$ for $k < k^-$ and $k > k^+$, both for the classical

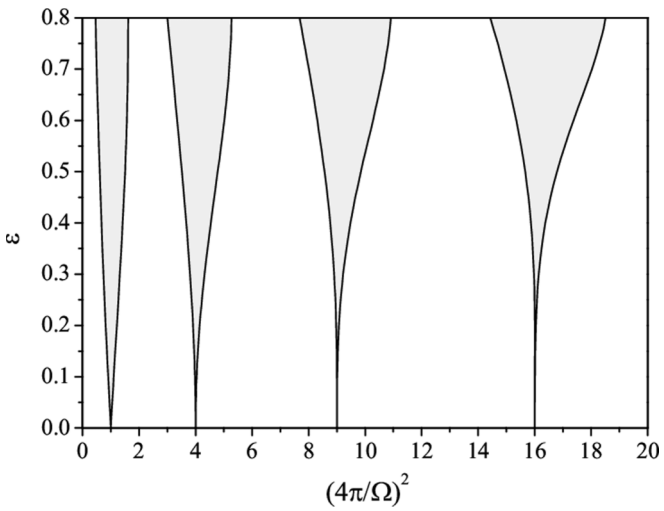

FIG. 4. The first four lacunae. The abscissa is $(4\pi/\Omega)^2$, which means that for $\varepsilon = 0$ at the resonance frequency $\Omega_n = 4\pi/n$ its value is n^2, for $n = 1, 2, 3, 4$.

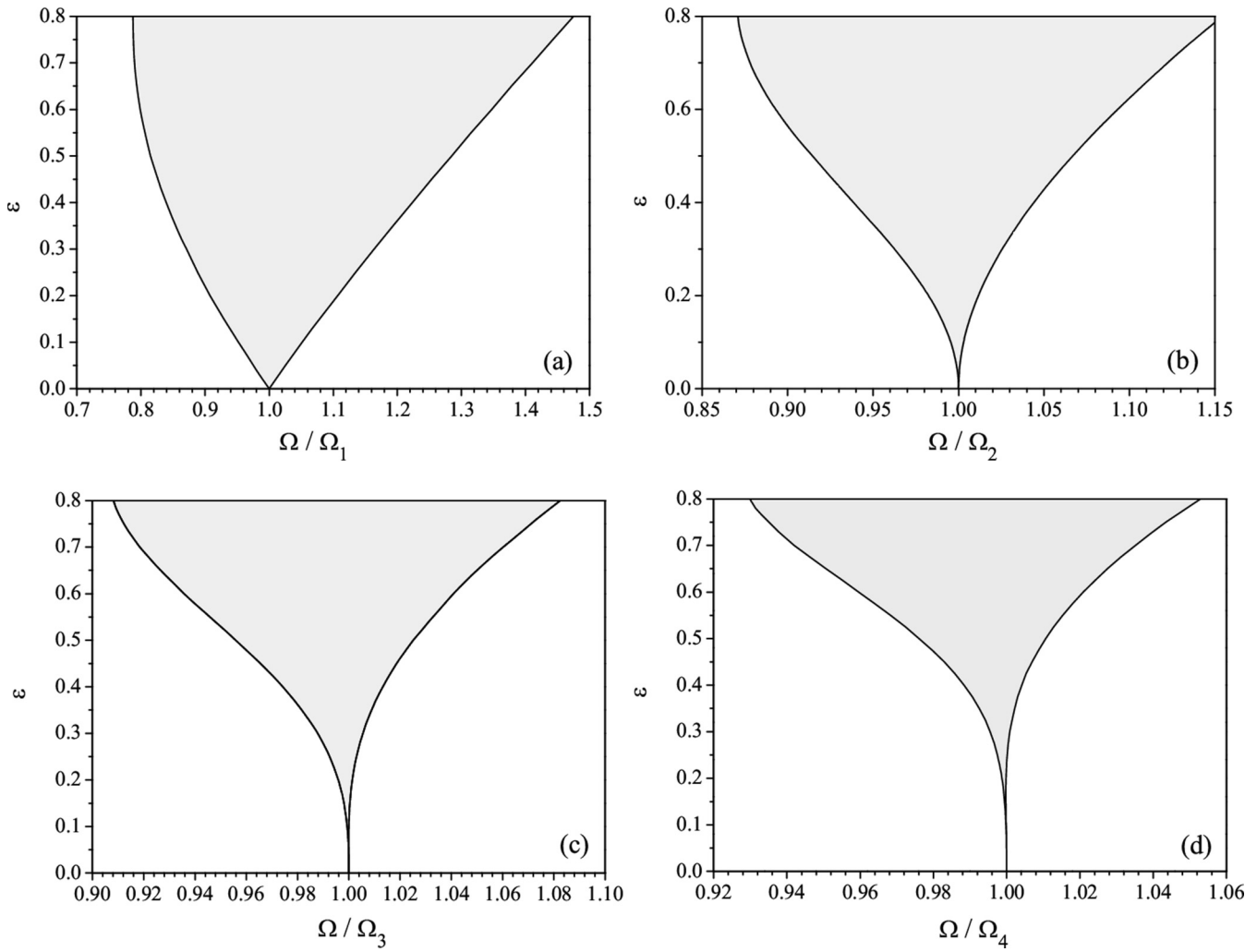

FIG. 5. The four lacunae $n = 1, 2, 3, 4$ in (a), (b), (c), and (d), respectively.

energy and the quantum energy, for $\varepsilon = 0.2$. As explained in the introduction we have to consider an ensemble of initial conditions to compare their average energy with the quantal average energy. In the case of the classical dynamics and to perform the statistical analysis, we have taken an ensemble of microcanonical initial conditions at $E_0 = I_0\omega_0$ (I_0 is the classical canonical action), where $\omega_0 = 2\pi(1+\varepsilon)$, and

$$x_0 = \sqrt{2I_0/\omega_0}\sin\theta, \quad p_0 = \sqrt{2I_0\omega_0}\cos\theta, \quad \theta \in [0, 2\pi], \tag{31}$$

where θ is assumed uniformly distributed over the interval $[0, 2\pi]$.

As is clearly seen, the lower and upper borders of the lacuna are very sharply determined, and the classical and quantum curves perfectly coincide, and thus have *exactly* identical boundary values k^-, k^+. In fact, we have used these observations to calculate the borders of lacunae for any ε and $n = 1, 2, 3, 4$, yielding the lacunae diagrams as presented in Figs. 4, 5, 6. To show the extreme accuracy of our procedure and the identity of the numerical classical and quantum borders of lacunae, we show in Table I the values for k^-, k^+ for $\varepsilon = 0.2, 0.4, 0.6, 0.8$.

V. MORE DETAILS ABOUT THE CLASSICAL DYNAMICS

It is interesting to study the dependence of the classical behavior on the initial conditions within the oscillatory (stable) regime, close to the instability border where $k < k^-$

TABLE I. The values for k^-, k^+ for $\varepsilon = 0.2, 0.4, 0.6, 0.8$.

k		$\varepsilon = 0.2$	$\varepsilon = 0.4$	$\varepsilon = 0.6$	$\varepsilon = 0.8$
k^-	Classical	0.90864958 ± 10^{-8}	0.83958033 ± 10^{-8}	0.79914257 ± 10^{-8}	0.78833642 ± 10^{-8}
	Quantum	0.90865 ± 10^{-5}	0.8396 ± 10^{-4}	0.7990 ± 10^{-4}	0.788 ± 10^{-3}
k^+	Classical	1.10653374 ± 10^{-8}	1.22299522 ± 10^{-8}	1.34602683 ± 10^{-8}	1.47354984 ± 10^{-8}
	Quantum	1.10653 ± 10^{-5}	1.2230 ± 10^{-4}	$1.3462 \pm 2 \cdot 10^{-4}$	1.474 ± 10^{-3}

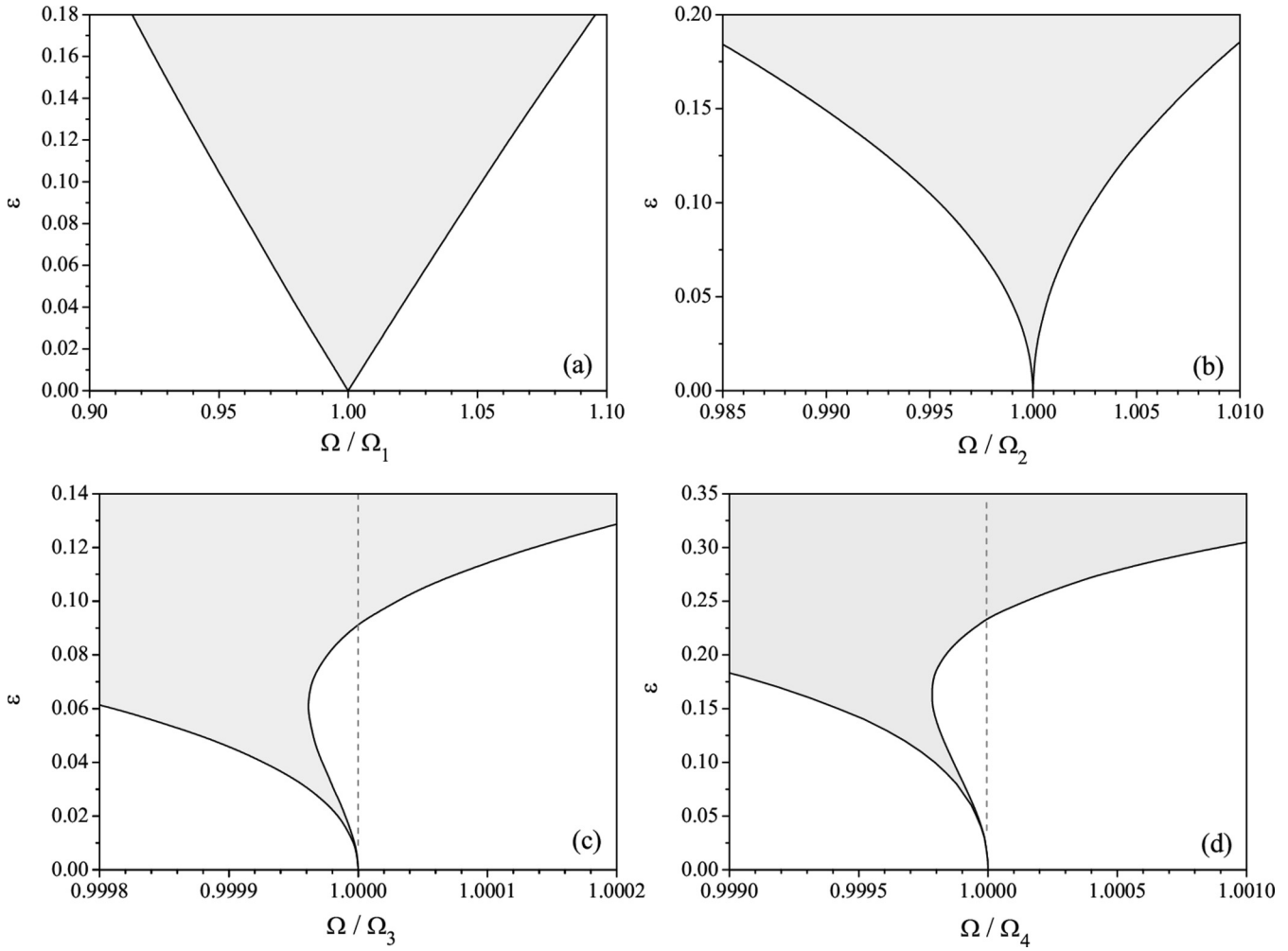

FIG. 6. The four lacunae $n = 1, 2, 3, 4$ in (a), (b), (c), and (d), respectively.

or $k > k^+$. This is shown in Fig. 8 for the first lacuna $n = 1$ and for fixed $\varepsilon = 0.2$.

The sensitive dependence of the oscillation on k is demonstrated in Fig. 9, where we fix $n = 1$, $\varepsilon = 0.2$, $x_0 = 0$, p_0 arbitrary, and for three values of $k = \Omega/\Omega_1 = \Omega/(4\pi)$. As is clearly seen, a minor deviation of k from $k^- = 0.9086496$ drastically changes the behavior of the system.

The border of lacuna is determined by the condition $|\mathrm{Tr}\Phi_1| = 2$, which at the given ε yields $k = k^-$ and

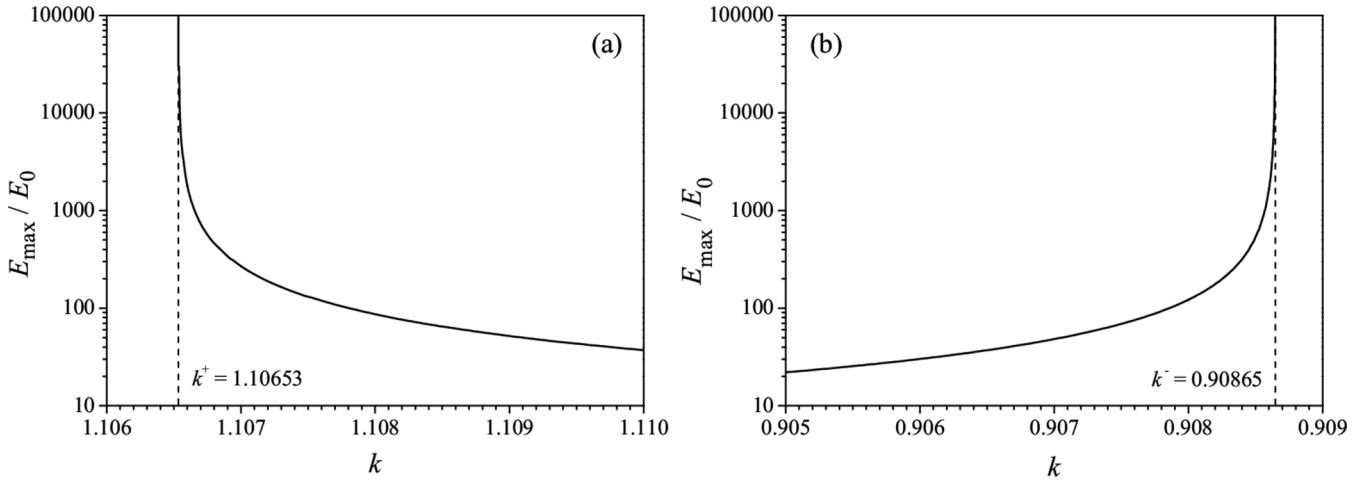

FIG. 7. The energy oscillation amplitude E_{max}/E_0 vs. $k > k^+$ in (a) and $k < k^-$ in (b) for $\varepsilon = 0.2$ and $n = 1$. We have verified that the classical and quantum curves perfectly coincide, which is another check of the accuracy of our numerical integrations.

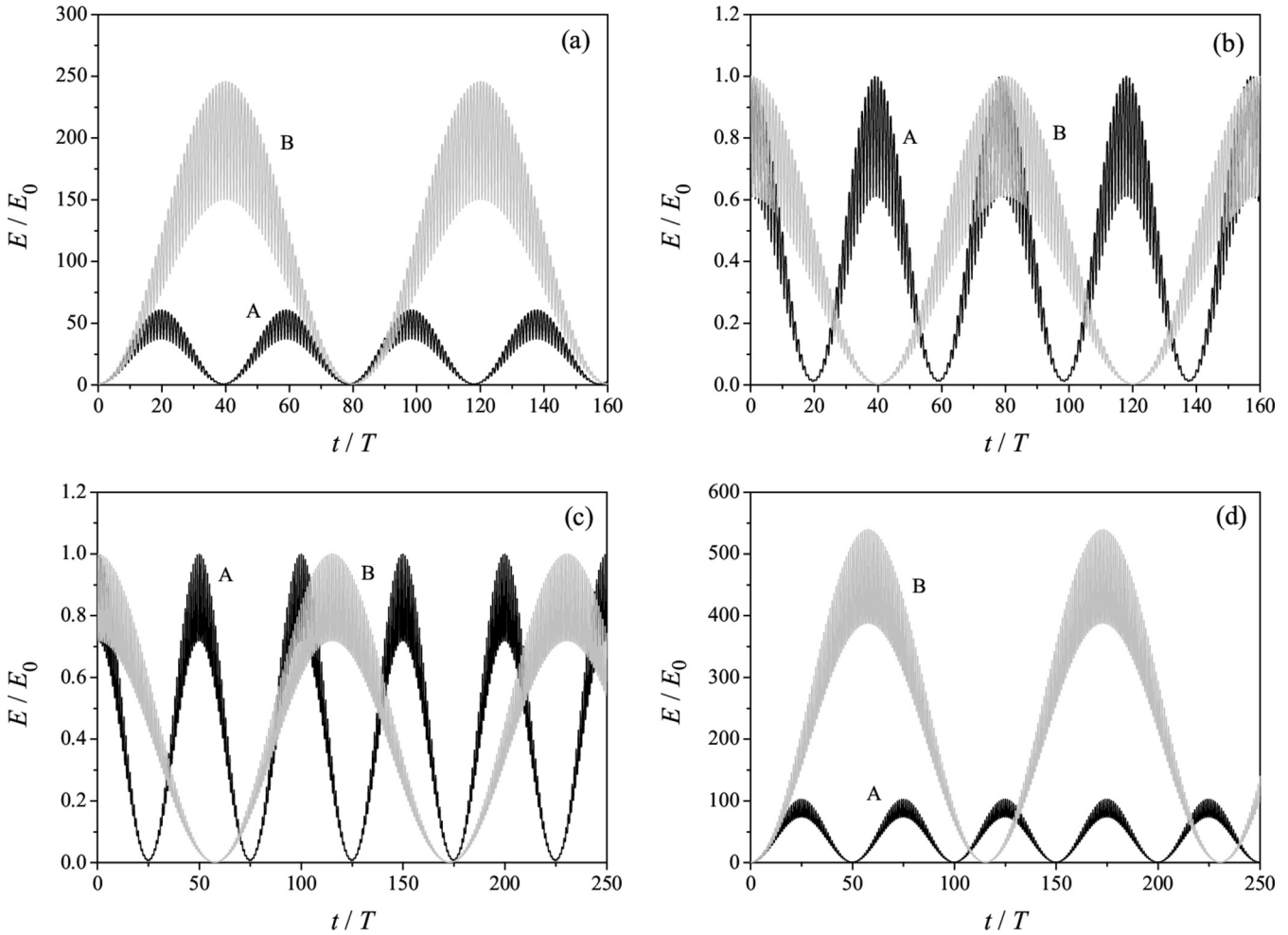

FIG. 8. Dependence of the oscillatory regime close to the border of the first lacuna $n = 1$ for $\varepsilon = 0.2$ on the initial conditions. In (a) and (c), x_0 is arbitrary and $p_0 = 0$. In (b) and (d), $x_0 = 0$ and p_0 arbitrary. In (a) and (b), $k^- = 0.90864958 \pm 10^{-8}$, and $k = 0.906$ in (A) and $k = 0.908$ in (B). In (c) and (d), $k^+ = 1.10653374 \pm 10^{-8}$, and $k = 1.109$ in (A) and $k = 1.107$ in (B).

$k = k^+$. Then calculating $\mathrm{Tr}\Phi$ as a function of time t gives an interesting behavior shown in Fig. 10 for the first lacuna $n = 1$ and various values of ε. Clearly, the curves are changing with t, but go through ± 2 at each integer multiple of $T = 2\pi/\Omega$.

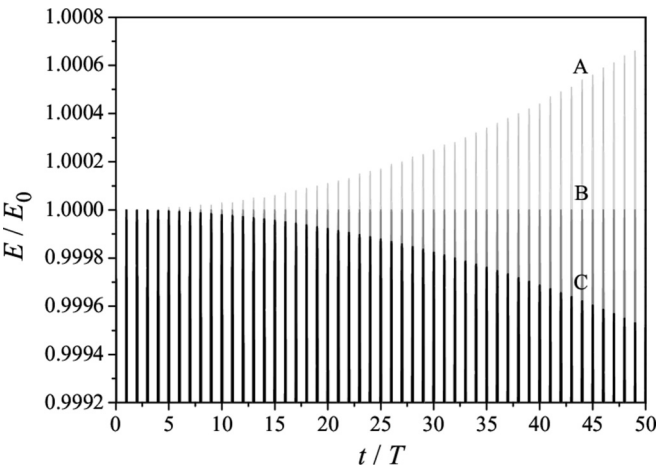

FIG. 9. Dependence of the oscillatory regime close to the border of the first lacuna $n = 1$ for $\varepsilon = 0.2$, for fixed initial conditions $x_0 = 0$, p_0 arbitrary: (A) $k = 0.9086497 > k^- = 0.9086496$, (B) $k = k^- = 0.9086496$, and (C) $k = 0.9086495 < 0.9086496$.

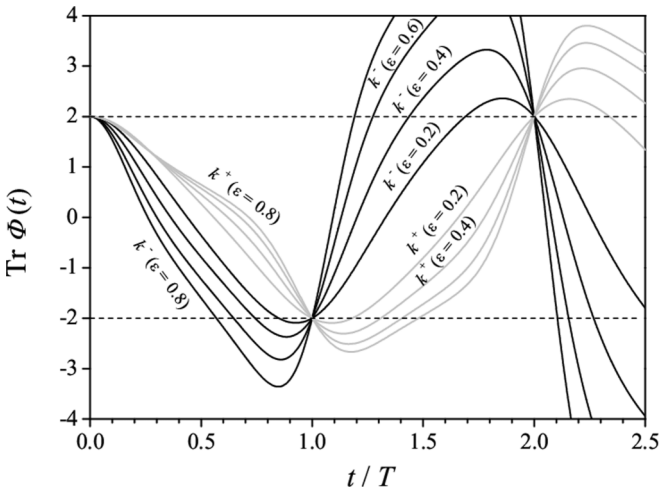

FIG. 10. $\mathrm{Tr}\Phi$ as a function of time t/T for $n = 1$ at various values of ε and corresponding values of k^+ and k^-. $\mathrm{Tr}\Phi(T) = -2$ for any single initial condition.

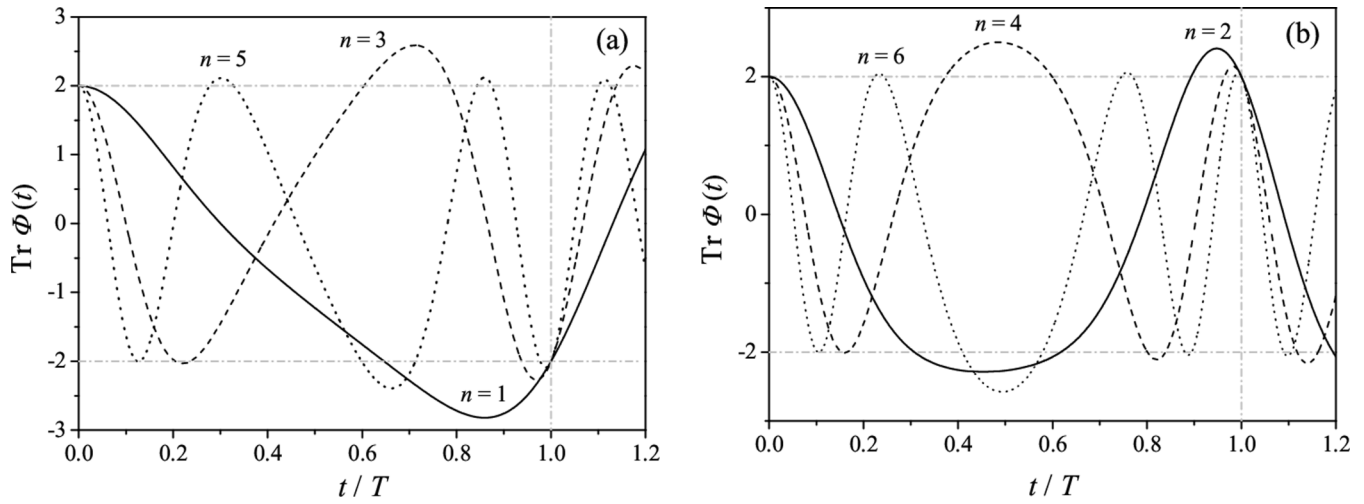

FIG. 11. TrΦ as a function of time t/T at fixed $\varepsilon = 0.6$ and $k = k^-$, for odd order lacunae $n = 1, 3, 5$ in (a) and even order lacunae $n = 2, 4, 6$ in (b). $\mathrm{Tr}\Phi(T) = -2$ for odd n and $\mathrm{Tr}\Phi(T) = 2$ for even n.

The same analysis has been done also for lacunae $n = 1, 2, \ldots, 6$ at fixed $\varepsilon = 0.6$ and corresponding $k = k^-$. The behavior is different for the odd and even n, as shown in Fig. 11. It is known [34] that the solution for certain single initial condition (x, p) is periodic with period T for $\mathrm{Tr}\Phi_1 = 2$, and periodic with period $2T$ when $\mathrm{Tr}\Phi_1 = -2$.

VI. COMPARISON OF THE UNSTABLE CLASSICAL AND QUANTUM DYNAMICS

From the stable and oscillatory regime we now turn to the unstable regime in lacunae and look more closely into the exponential growth of the energy. Here the numerical effort is extreme, because due to the exponential growth the coefficients $b_m(t)$ from Eq. (12) grow quickly, and therefore to warrant the necessary numerical accuracy, it is necessary to take very large truncation order M. In Fig. 12 we show the results for the first lacuna $n = 1$, both classically and quantally, for $k = 1$, which means $\Omega = \Omega_1 = 4\pi$, and for various ε. The two curves coincide exactly. The growth of the energy, starting from the initial energy E_0, is oscillatory, but in the mean exponential. The same analysis has been performed also for the second lacuna $n = 2$, presented in Fig. 13. In both cases the classical curve is obtained as the average over the microcanonical ensemble of initial conditions. The fact that the quantum and classical curves perfectly coincide is another, the crucial test of the numerical accuracy.

VII. EMPIRICAL RESULTS CHARACTERIZING THE STRUCTURE OF INSTABILITY REGIONS (LACUNAE)

As described in Secs. II C and IV we have established the identity of the classical and quantal borders of lacunae. Inside the lacunae the energy $E(t)$ grows exponentially, in the

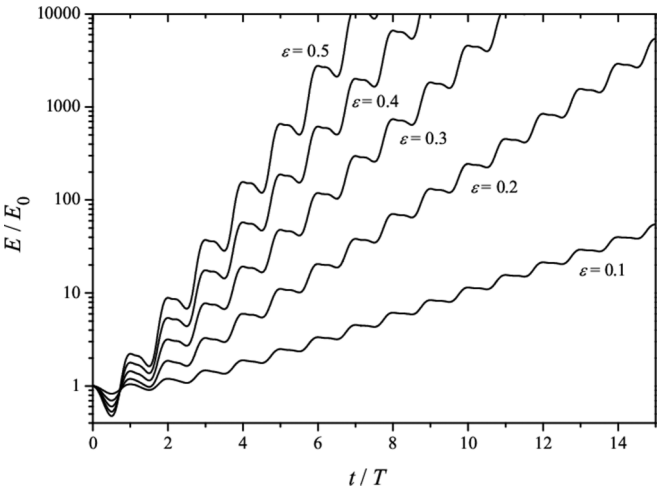

FIG. 12. Exponential growth of the energy $E(t)$ starting at E_0, quantally and classically (they coincide perfectly), for $n = 1$, $k = 1$, $M = 45\,000$ and integration step size $h = 2 \times 10^{-6}$, for $\varepsilon = 0.1, 0.2, 0.3, 0.4$, and 0.5. The classical curve is for the mean value over the microcanonical ensemble of initial conditions with E_0.

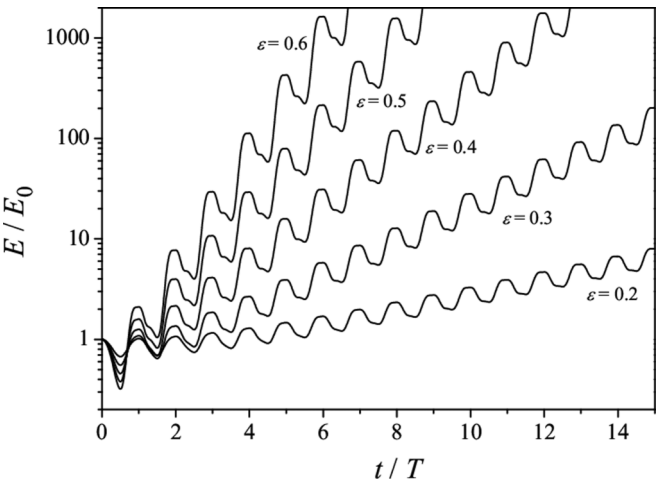

FIG. 13. Exponential growth of the energy $E(t)$ starting at E_0, quantally and classically (they coincide perfectly), for $n = 2$, $k = 1$, $M = 10\,000$ and integration step size $h = 10^{-5}$, for $\varepsilon = 0.1, 0.2, 0.3, 0.4$, and 0.5. The classical curve is for the mean value over the microcanonical ensemble of initial conditions with E_0.

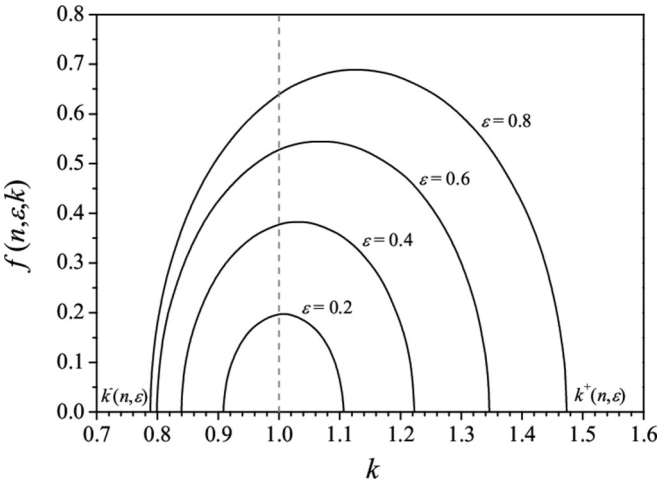

FIG. 14. Plot of the exponent $f(n, \varepsilon, k)$ from the elliptic Eq. (33) for the first lacuna $n = 1$.

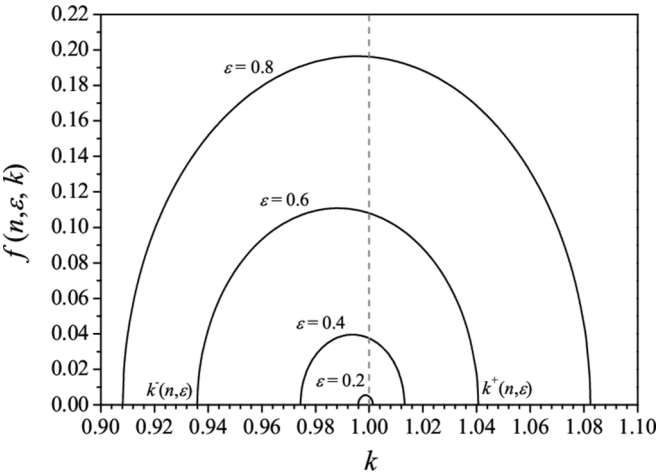

FIG. 16. Plot of the exponent $f(n, \varepsilon, k)$ from the elliptic Eq. (33) for the third lacuna $n = 3$.

classical case as follows:

$$\frac{E(t)}{E_0} = F(n, \varepsilon, k, x_0, p_0) \exp[2\pi\ f(n, \varepsilon, k)\, t], \tag{32}$$

which is valid for sufficiently large time t, as demonstrated in the previous Sec. VI. Of course, the values of $E(t)$ in Eq. (32) are taken for the tangent of the curve as seen, e.g., in Figs. 12 and 13, thereby eliminating the oscillations of $E(t)$ around the mean straight line. It turns out that the energy growth exponent $f(n, \varepsilon, k)$ as defined above is empirically well approximated with high (maximal) accuracy by the empirical value $f_e(n, \varepsilon, k)$ satisfying the following equation of the elliptic type,

$$\frac{(k - k_0)^2}{k_a^2} + \frac{f_e^2}{f_{\max}^2} = 1, \tag{33}$$

where we define

$$k_0 = \tfrac{1}{2}(k^+ + k^-), \quad k_a = \tfrac{1}{2}(k^+ - k^-), \quad f_{\max} = f(k_0). \tag{34}$$

Thus the solution of Eq. (33) gives an excellent approximation for $f(n, \varepsilon, k)$, namely,

$$f_e(n, \varepsilon, k) = f_{\max}(n, \varepsilon)\sqrt{1 - \frac{(k - k_0)^2}{k_a^2}}. \tag{35}$$

Within the accuracy of plots in Figs. 14, 15, and 16, for the lacunae $n = 1, 2, 3$, respectively, the empirical formula Eq. (33) is fully obeyed. Moreover, since we believe that this empirical finding is very important, we want to present the accuracy, the errors $f_e(n, \varepsilon, k) - f(n, \varepsilon, k)$, quantitatively in Table II. We see that the error is within the range 2×10^{-5} and 10^{-4}, which indicates that probably the Eq. (33) is an exact law, and therefore it is a challenge to derive it theoretically, using, e.g., WKB method [32,38], convenient to tackle the problem of parametric resonance.

We have also tried to find a simple law for $f_{\max}(n, \varepsilon)$ as a function of ε, for various $n = 1, 2, 3 \ldots$, but no simple analytic expression could be found to fit the data so far.

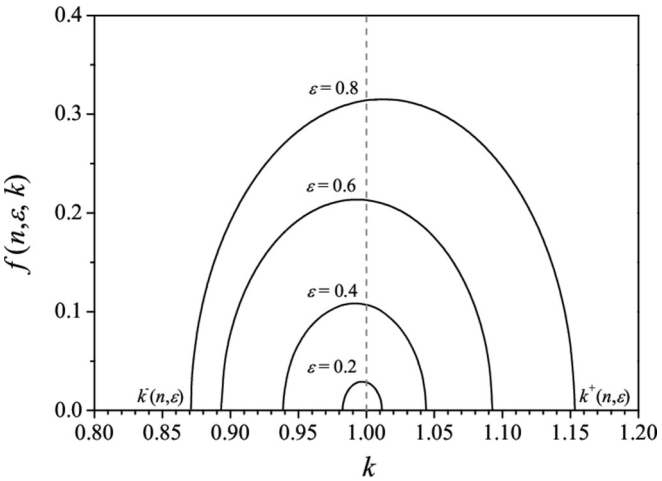

FIG. 15. Plot of the exponent $f(n, \varepsilon, k)$ from the elliptic Eq. (33) for the second lacuna $n = 2$.

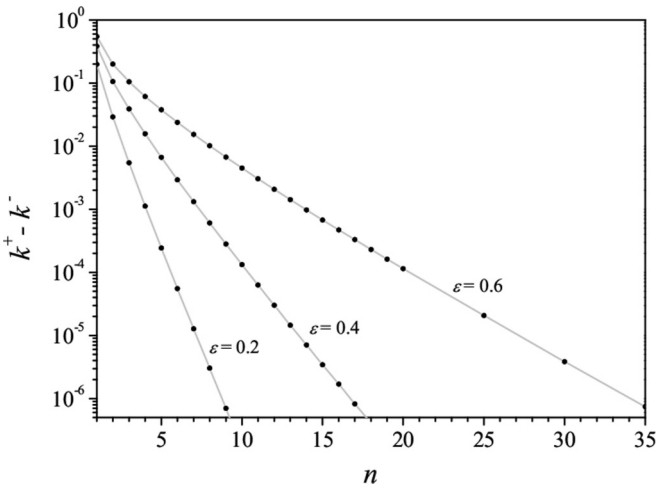

FIG. 17. The width of the lacunae $k^+ - k^-$ at fixed $\varepsilon = 0.2, 0.4, 0.6$ decays exponentially with the order n of the lacunae.

TABLE II. The accuracy of the empirical Eq. (33). See text.

$\varepsilon = 0.2$				$\varepsilon = 0.4$			
$k^- = 0.90864958 \pm 10^{-8}$				$k^- = 0.83958033 \pm 10^{-8}$			
$k^+ = 1.10653374 \pm 10^{-8}$				$k^+ = 1.22299522 \pm 10^{-8}$			
$f_{\max} = 0.19767 \pm 2 \times 10^{-5}$				$f_{\max} = 0.38269 \pm 2 \times 10^{-5}$			
k	$f_e(n,\varepsilon,k)$ $\pm 2 \times 10^{-5}$	$f(n,\varepsilon,k)$ $\pm 2 \times 10^{-5}$	$f_e - f$ $\pm 2 \times 10^{-5}$	k	$f_e(n,\varepsilon,k)$ $\pm 5 \times 10^{-5}$	$f(n,\varepsilon,k)$ $\pm 5 \times 10^{-5}$	$f_e - f$ $\pm 5 \times 10^{-5}$
0.92	0.09193	0.09194	−0.00001	0.85	0.12445	0.12457	−0.00012
0.94	0.14436	0.14437	−0.00001	0.86	0.17186	0.17201	−0.00015
0.96	0.17330	0.17331	−0.00001	0.88	0.23504	0.23521	−0.00017
0.98	0.18983	0.18984	−0.00001	0.90	0.27887	0.27902	−0.00015
1.00	0.19709	0.19710	−0.00001	0.95	0.34658	0.34668	−0.00010
k_0	0.19767	0.19767	0.00000	1.00	0.37756	0.37759	−0.00003
1.02	0.19611	0.19611	0.00000	k_0	0.38269	0.38269	0.00000
1.04	0.18677	0.18677	0.00000	1.05	0.38086	0.38085	0.00001
1.06	0.16766	0.16766	0.00000	1.10	0.35726	0.35722	0.00004
1.08	0.13471	0.13471	0.00000	1.15	0.30049	0.30041	0.00008
1.10	0.07064	0.07063	0.00001	1.20	0.18173	0.18167	0.00006
				1.22	0.06738	0.06736	0.00002
$\varepsilon = 0.6$				$\varepsilon = 0.8$			
$k^- = 0.79914257 \pm 10^{-8}$				$k^- = 0.78833642 \pm 10^{-8}$			
$k^+ = 1.34602683 \pm 10^{-8}$				$k^+ = 1.47354984 \pm 10^{-8}$			
$f_{\max} = 0.54720 \pm 2 \times 10^{-5}$				$f_{\max} = 0.68919 \pm 2 \times 10^{-5}$			
k	$f_e(n,\varepsilon,k)$ $\pm 5 \times 10^{-5}$	$f(n,\varepsilon,k)$ $\pm 10^{-4}$	$f_e - f$ $\pm 10^{-4}$	k	$f_e(n,\varepsilon,k)$ $\pm 5 \times 10^{-5}$	$f(n,\varepsilon,k)$ $\pm 10^{-4}$	$f_e - f$ $\pm 10^{-4}$
0.81	0.15266	0.1537	−0.0011	0.79	0.06783	0.0693	−0.0014
0.85	0.31784	0.3195	−0.0016	0.80	0.17830	0.1818	−0.0035
0.90	0.42444	0.4259	−0.0015	0.90	0.50908	0.5140	−0.0049
0.95	0.48913	0.4902	−0.0011	1.00	0.63687	0.6396	−0.0027
1.00	0.52757	0.5281	−0.0006	1.10	0.68637	0.6869	−0.0005
k_0	0.54720	0.5472	0.0000	k_0	0.68919	0.6892	0.0000
1.10	0.54444	0.5443	0.0001	1.20	0.67504	0.6740	0.0010
1.15	0.52481	0.5245	0.0004	1.30	0.59944	0.5976	0.0019
1.20	0.48416	0.4836	0.0006	1.40	0.42667	0.4248	0.0019
1.25	0.41639	0.4157	0.0006	1.47	0.09895	0.0985	0.0005
1.30	0.30384	0.3033	0.0006				
1.34	0.11425	0.1140	0.0002				

Finally, we have investigated how the width of the lacuna $k^+ - k^-$ changes with the order n of the lacuna, at fixed ε. The result is shown in Fig. 17 for three different values of $\varepsilon = 0.2, 0.4, 0.6$. It is clearly seen that the width of the lacunae (at fixed ε) decreases exponentially with n, in agreement with some asymptotic results [32], valid if $\omega(t)$ is an analytic periodic function of time t. More results based on the WKB method are expected [38]. The results are consistent with the theorems 2.2. and 2.13 in Ref. [35].

VIII. DISCUSSION AND CONCLUSIONS

We have studied the parametric resonance of the quantum and classical linear oscillator with the specific periodic driving law, where the oscillation frequency (rather than its square) changes harmonically with time as $\omega(t) = 2\pi(1 + \varepsilon \cos \Omega t)$. This enables certain technical simplifications. Our analysis is classical and quantal, theoretical and numerical. We are using the Runge-Kutta method of fourth order, with a number of careful checks of the necessary and sufficient accuracy. We have investigated the regions of exponential instability (called lacunae) in the control parameter space (Ω, ε) and determined the borders of lacunae, and we have studied in detail the stable oscillatory dynamical regime outside lacunae, as well as the exponential growth inside the lacunae. The most important finding is the fact, explained in Secs. II C and IV, that the borders of lacunae classically and quantally *exactly* coincide. This is due to the fact that the quantum propagator can be exactly and explicitly expressed in terms of the classical propagator. As a consequence of that the evolution of the quantum energy expectation value can be calculated for an arbitrary normalizable initial state, and for the special case of an initial pure stationary eigenstate the evolution is exactly equal to the evolution of the energy of the classical microcanonical ensemble of initial conditions of the same starting energy. In nonlinear systems such correspondence can be expected only at large energies and quantum numbers (short wavelength approximation). We have also found an important empirical

relationship, an equation of elliptic type, which determines the exponent of the energy growth in terms of other system's parameters, and seems to be an exact law, still open as a challenge for a theoretical derivation (proof). We believe that our approach is suitable for other similar Floquet systems, where we expect qualitatively similar conclusions. As for the quantum mechanics of our system, it is clear that the Floquet operator (Φ_1) (see Sec. II) must have continuous spectrum inside the lacunae, and discrete spectrum outside the lacunae, but it is difficult to calculate the spectrum in general, although one remarkable exact result has been obtained by Weigert [33] for a quite special but nevertheless representative system. For more related comments see [42] and the review paper by Casati and Molinari [43].

We think that more numerical and analytical studies should be initiated in this direction, to study the linear Floquet systems, probably using the WKB method [32]. Parametric periodic driving of nonlinear systems shows an even more complicated structure, including the chaotic behavior, such as exemplified by, e.g., quantum and classical kicked rotator [14,43,44] or quartic oscillator [6], etc.

ACKNOWLEDGMENTS

Financial support of the Slovenian Research Agency ARRS under Grant No. P1-0306 is gratefully acknowledged. M.R. acknowledges the support by the Department of Mathematics of Huaqiao University during the research stay there. This work was partially supported by the National Natural Science Foundation of China under Grant No. 11671176, and the Natural Science Foundation of Zhejiang Province under Grant No. LY15A010007. We thank Mr. Martin Vogrin (University of Hamburg) for cooperation at the initial stage of this work.

[1] V. I. Arnold, *Mathematical Methods of Classical Mechanics* (Springer-Verlag, New York, 1980).
[2] P. Lochak and C. Meunier, *Multiphase Averaging for Classical Systems* (Springer-Verlag, New York, 1988).
[3] G. M. Zaslavsky, *The Physics of Chaos in Hamiltonian Systems* (Imperial College Press, London, 2007).
[4] E. Ott, *Chaos in Dynamical Systems* (Cambridge University Press, Cambridge, 1993).
[5] B. V. Chirikov, Phys. Rep. **52**, 263 (1979).
[6] G. Papamikos and M. Robnik, J. Phys. A: Math. Theor. **44**, 315102 (2011).
[7] G. Papamikos, B. C. Sowden, and M. Robnik, Nonlin. Phenom. Complex Syst. (Minsk) **15**, 227 (2012).
[8] B. Batistić and M. Robnik, J. Phys. A: Math. Theor. **44**, 365101 (2011).
[9] B. Batistić and M. Robnik, in *Eighth International Summer School/Conference on Let's Face Chaos Through Nonlinear Dynamics*, edited by M. Robnik and V. G. Romanovski, AIP Conf. Proc. No. 1468 (AIP, Melville, NY, 2012), p. 297.
[10] B. Liebchen, R. Buchner, C. Petri, F. K. Diakonos, F. Lenz, and P. Schmelcher, New J. Phys. **13**, 093039 (2011).
[11] D. Andresas and M. Robnik, J. Phys. A: Math. Theor. **47**, 355102 (2014).
[12] D. Andresas, B. Batistić, and M. Robnik, Phys. Rev. E. **89**, 062927 (2014).
[13] P. Schmelcher, F. Lenz, D. Matrasulov, Z. A. Sobirov, and S. K. Avazbaev, Complex phenomena in nanoscale systems, in *Proceedings of the NATO Science for Peace and Security Series B: Physics and Biophysics*, edited by G. Casati and D. Matrasulov (Springer, Dordrecht, 2009).
[14] T. Manos and M. Robnik, Phys. Rev. E **87**, 062905 (2013).
[15] B. Batistić, T. Manos, and M. Robnik, Europhys. Lett. **102**, 50008 (2013).
[16] V. Grubelnik, M. Logar, and M. Robnik, J. Phys. A: Math. Theor. **47**, 355103 (2014).
[17] J. V. Jose and R. Cordery, Phys. Rev. Lett. **56**, 290 (1986).
[18] V. V. Dodonov, A. B. Klimov, and D. E. Nikonov, J. Math. Phys. **34**, 3391 (1993).
[19] A. J. Makowski and S. T. Dembinski, Phys. Lett. A **154**, 217 (1991).
[20] A. J. Makowski, J. Phys. A: Math. Gen. **25**, 3419 (1992).
[21] C. Li, Chinese Phys. Lett. **25**, 1545 (2008).
[22] P. Seba, Phys. Rev. A **41**, 2306 (1990).
[23] F. Lenz, B. Liebchen, F. K. Diakonos, and P. Schmelcher, New J. Phys. **13**, 103019 (2011).
[24] J. Liss, B. Liebchen, and P. Schmelcher, Phys. Rev. E **87**, 012912 (2013).
[25] S. Gehler, T. Tudorovskiy, Schindler, U. Kuhl, and H.-J. Stockmann, New J. Phys. **15**, 083030 (2013).
[26] S. D. Martino, F. Anza, P. Facchi, A. Kossakowski, G. Marmo, A. Messina, B. Militello, and S. Pascazio, J. Phys. A: Math. Theor. **46**, 365301 (2013).
[27] E. Fermi, Phys. Rev. **75**, 1169 (1949).
[28] S. M. Ulam, *Proceedings of the Fourth Berkeley Symposium on Mathematical Statistics and Probability* (University of California, Berkeley, 1961).
[29] A. J. Lichtenberg and M. A. Lieberman, *Regular and Chaotic Dynamics* (Springer, New York, 2010).
[30] C. Scheininger and M. Kleber, Physica D **50**, 391 (1991).
[31] G. Karner, J. Statisical Phys. **77**, 867 (1994).
[32] M. V. Fedoryuk, *Asymptotic Analysis* (Springer-Verlag, Berlin, 1993).
[33] S. Weigert, J. Phys. A: Math. Theor. **35**, 4169 (2002).
[34] N. W. McLachlan, *Theory and Applications of Mathieu Functions* (Dover Publications, New York, 1964).
[35] W. Magnus and S. Winkler, *Hill's Equation* (Interscience Publishers, New York, 1966).
[36] A. H. Nayfeh and D. T. Mook, *Nonlinear Oscillations* (John Wiley, New York, 1979).
[37] M. Combescure and D. Robert, Asymptot. Anal. **14**, 377 (1997).

[38] M. Robnik (unpublished).
[39] M. Robnik and V. G. Romanovski, J. Phys. A: Math. Theor. **39**, L35 (2006).
[40] M. Robnik and V. G. Romanovski, Open Syst. Info. Dynam. **13**, 197 (2006).
[41] *Seventh International Summer School/Conference on Let's Face Chaos Through Nonlinear Dynamics*, edited by M. Robnik and V. G. Romanovski, AIP Conf. Proc. No. 1076 (AIP, Melville, NY, 2008).
[42] K. Yajima and H. Kitada, Ann. l'Inst. Henri Poincare **39**, 145 (1983).
[43] G. Casati and L. Molinari, Prog. Theor. Phys. Suppl. **98**, 287 (1989).
[44] F. M. Izrailev, Phys. Rep. **196**, 299 (1990).